Mechanism and Kinetics of Oligosilsesquioxane Growth in the In Situ Water Production Sol–Gel Route: Dependence on Water Availability

Evgeny Borovin, Emanuela Callone, François Ribot, Sandra Diré

Mechanism and kinetics of oligosilsesquioxanes growth in the ISWP sol-gel route: dependence on the water availability

Evgeny Borovin*[a], Emanuela Callone[a], Francois Ribot[b] and Sandra Diré*[a]

[a] Department of Industrial Engineering - University of Trento - via Sommarive 9 - 38123, Trento, Italy

E-mail: evgeny.borovin@unitn.it, sandra.dire@unitn.it

[b] Laboratoire de Chimie de la Matière Condensée de Paris (LCMCP) - Sorbonne Universités, UPMC Univ Paris 06, CNRS, Collège de France - 11 place Marcelin Berthelot, F-75005 Paris, France

Abstract: Thiol functionalized nanobuilding blocks (NBBs) have been synthesized from 3-mercaptopropyltrimethoxysilane, using the in-situ water production (ISWP) process in which the water needed to hydrolyze the precursor was provided via an esterification reaction. In the present study the reaction between 1-propanol and chloroacetic acid was used. While the growth of the Si oligomers has been followed at room temperature and 100 °C with 1D ^{29}Si and 2D ^{1}H-^{29}Si HSQC NMR experiments, the amount of water delivered along the process was followed by ^{1}H NMR. The results show a good correlation between the evolution of the degree of condensation and the amount of water produced in situ. They also point out the preferential formation of cage-like structures and the narrowing of the species distribution at long reaction time. The average size of the growing oligomers was estimated from their diffusion coefficient that was measured by ^{1}H diffusion-ordered NMR spectroscopy (DOSY NMR). Like gel permeation chromatography, DOSY NNR shows a plateau between 70 to 100 hours in the growth of the oligomers, a time when, according to ^{29}Si NMR, the well-defined octakis(3-mercaptopropylsilsesquioxane) is the major species.

Introduction

Hybrid organic/inorganic materials are highly promising multifunctional materials in a vast area of applications.[1-3] They have been widely exploited during the last decade thanks to the structural flexibility and possibility of controlling their structure on the nanometric scale. Many strategies can be followed in order to prepare such hybrids.[4] Among them, sol-gel process is a well-established one and allows preparation of homogeneous hybrids starting from alkoxide precursors and using hydrolysis-condensation reactions. The organoalkoxysilanes of the type $R_nSi(OR')_{4-n}$, with various R organic functional groups and OR' alkoxy groups, are well-known as precursors for the preparation of silica-based organic/inorganic hybrids.[1,2] Silsesquioxanes prepared via hydrolysis-condensation of organoalkoxysilanes find applications among the most popular commercial sol–gel products, particularly in the field of coatings.[5] A number of studies were carried on different organically modified alkoxysilanes, where their pre-hydrolysis step usually initiates the network formation.[6-20] However in the case of conventional hydrolytic sol-gel synthesis some negative aspects such as local inhomogeneity and low crosslinking degree of the final material structure are often unavoidable.[21] In order to overcome these negative aspects, the nanobuilding blocks (NBBs) approach can be used for hybrids preparation,[1,22,23] thus preserving initial structural features during the formation of the final material and allowing to fine tune the properties.[24,25] As we reported recently the NBBs synthesis is achievable under strictly controlled conditions exploiting in situ water production (ISWP) provided by the esterification reaction between a carboxylic acid and an alcohol. These reactions were compared in terms of the influence of the chosen reagents on the condensation degree and the product structure.[26,27]

In this paper we report on the structural development and growth mechanisms of NBBs prepared by the ISWP route from 3-mercaptopropyltrimethoxysilane (McPTMS). This starting precursor, with its thiol function is interesting for different applications, ranging from the immobilization on the hybrid surface of bio-molecules, such as enzymes or proteins[28] and transition metals,[29] to the development of bio-sensing[30] and peptide separation[31] devices. All these applications require particular control of the availability and reactivity of the SH functions in the final hybrids. ^{1}H NMR, ^{29}Si NMR, Pulsed Field Gradient Spin Echo ^{1}H NMR (DOSY), Gel Permeation Chromatography and FTIR techniques were combined to yield a deeper insight on the chemical composition and structural network development in relation with reaction time. Optimization of the hydrolysis-condensation extent, with preferential

cage-like and ladder-like small oligomers formation, was reached by time-dependent monitoring of two different temperature conditions: room temperature and 100 °C.

Results and Discussion

Alkoxysilanes hydrolysis-condensation kinetics is known to depend, among other factors, on the H_2O availability in the reacting system.[5,32,33] In the ISWP route used in the present work, the water is generated in situ by the esterification reaction between chloroacetic acid and 1-propanol (Figure 1, reaction a). The water availability depends on the kinetics of reaction a, which is affected, apart from other factors, by the temperature. Moreover, as the alcohol used is 1-propanol but the precursor introduced is a trimethoxy, transalcoholysis can also take place (Figure 1, reaction b). It yields new alkoxysilane precursors, of general formula $HSCH_2CH_2CH_2Si(OMe)_{3-n}(OPr)_n$ (with n = 1,2 or 3), and free methanol that can be involved both in an esterification reaction, similar to (a), and in a transesterification reaction (Figure 1, reaction c). All these reactions are simultaneous and interconnected in the means of their reagent-products interaction and reactions kinetics, thus the influence of such a system on the hydrolysis-condensation of McPTMS is complex.

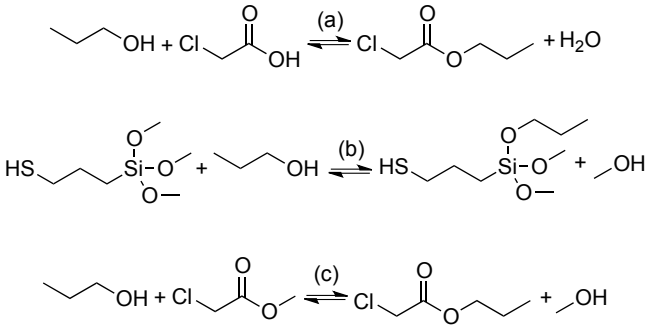

Figure 1. Esterification (a), transalkoholysis (b) and transesterification (c) reactions occurring in the reaction mixture.

To follow the structural development and the growth of NBBs in situ, ^{29}Si NMR spectra were acquired for solutions reacted at room temperature or 100 °C after different times ranging from 0.5 to 380 hours. Figure 2 presents a selection of ^{29}Si DEPT NMR spectra acquired during the first 72 hours of reaction at room temperature.

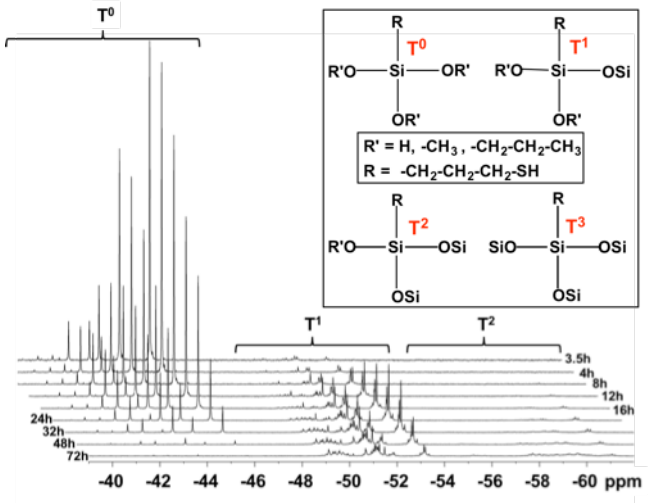

Figure 2. ^{29}Si DEPT NMR spectra of thiol functionalized NBBs obtained by mixing McPTMS, PrOH, ClAA and DBTL (1:18:6:0.015) after various times at RT. T-units structures are shown for reference.

The sharp signals between -39 and -46 ppm reflect all the T^0 units generated in the reaction medium from McPTMS by transalcoholysis (reaction b) and hydrolysis. Their general formula is $HSCH_2CH_2CH_2Si(OMe)_n(OPr)_p(OH)_{3-(n+p)}$ with *n* and *p* equal to 0, 1, 2 or 3 (but $n+p \leq 3$). The replacement of Si-OR or Si-OH moieties by Si-O-Si link, that occurs upon condensation, is known to cause a high field shift for each additional siloxane bridge.[34] Accordingly, the more complex and overlapping signals that grow with time between -48 and -54 ppm correspond to T^1 sites (*i.e.* Si with just one Si-O-Si link), while the weak ones that start to appear after 16 hours between -55 and -62 ppm are associated to T^2 environments (*i.e.* Si with two Si-O-Si links). No further condensed T^3 sites (*i.e.* Si with three Si-O-Si links) are observed after 72 hours at room temperature. According to the very small amount of T^2 sites, most of the T^1 signals are related to dimers of general formula $RSi(OPr)_n(OMe)_p(OH)_{2-(n+p)}$-O-$Si(OPr)_{n'}(OMe)_{p'}(OH)_{2-(n'+p')}R$, where R stand for $-CH_2CH_2CH_2SH$ and *n*, *p*, *n'* and *p'* equal 0, 1, or 2 (but $n+p \leq 2$ and $n'+p' \leq 2$). When *n* equals *n'* and *p* equals *p'*, the corresponding dimers are symmetric and give rise to one signal, whereas in all other cases two signals are expected.

With the help of the time evolution of the T^0 signals and ^1H-^{29}Si HSQC (or HMBC) experiments, that allow correlating a given Si signal with the proton signals of $-OCH_3$ or $-OCH_2-$ moieties attached to this silicon, a complete assignment of the T^0 region was possible. It is schematically presented in Figure 3. The substitution of an alkoxy group by a hydroxyl group induces a conventional downfield shift [33] in the ranges 0.9 - 0.6 ppm and 2.2 - 1.8 ppm for methoxy and propoxy replacement, respectively. This downfield shift decreases with the increase of hydrolysis ratio. Such effect can be traced to steric interaction, as previously described.[35] On the contrary, the high field shifts observed upon substituting a methoxy group by a propoxy group equals 1.26 ± 0.02 ppm, regardless of the amount of hydroxyl groups in the monomers.

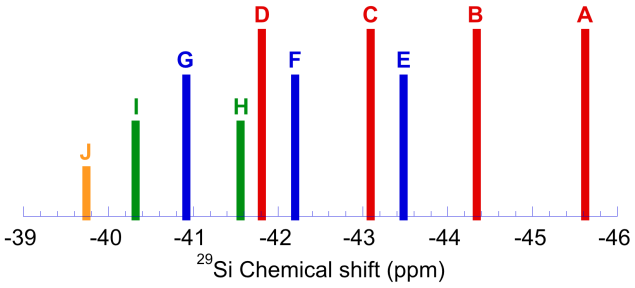

Figure 3. ^{29}Si NMR chemical shifts for the ten T^0 species that can be generated upon mixing McPTMS, PrOH and ClAA. A: $RSi(OPr)_3$, B: $RSi(OPr)_2(OMe)$, C: $RSi(OPr)(OMe)_2$, D: $RSi(OMe)_3$ (i.e. McPTMS), E: $RSi(OPr)_2(OH)$, F: $RSi(OPr)(OMe)(OH)$, G: $RSi(OMe)_2(OH)$, H: $RSi(OPr)(OH)_2$, I: $RSi(OMe)(OH)_2$, and J: $RSi(OH)_3$ (R = $-CH_2CH_2CH_2SH$).

A stack plot of ^{29}Si DEPT NMR spectra is shown in Figure 4 for the first 48 hours at 100 °C. Peaks are spread in four main separated groups. They reflect the condensation reactions and can be assigned as follow: T^0 (from -39 to -46 ppm), T^1 (from -48 to -54 ppm), T^2 (from -54 to -63 ppm), T^3 (from -63 to -70 ppm). Figure 4 highlights the changes that species undergo during the reaction: the gradual disappearance of T^0 and T^1 units, the recombination of T^2 units and the formation of T^3 units, among which the most intense peak at -66.7 ppm can be attributed to the $[T_3]_8$ cage.[36] As expected, the reactions proceed much faster than at room temperature and a higher degree of condensation is reached. After only 0.5 hour, some T^2 sites are already observed, indicating the rapid formation of trimers or oligomers of higher nuclearity, but the main species are still dimers. After 48 hours, only T^2 and T^3 sites are observed, indicating the total disappearance of dimers.

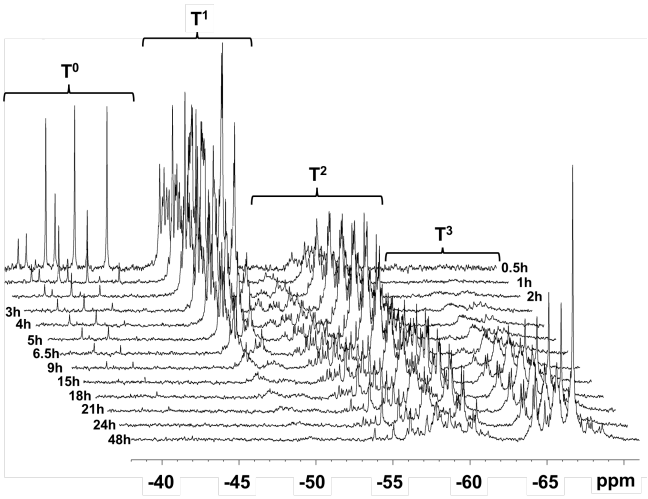

Figure 4. ^{29}Si DEPT NMR spectra of thiol functionalized NBBs obtained by mixing McPTMS, PrOH, ClAA and DBTL (1:18:6:0.015) after various times at 100 °C.

As DEPT introduces a different transfer function for each environment, quantification requires the assignment of each signal and is therefore tedious and not straightforward.[32] Yet, comparison of the T^n relative integrals of ^{29}Si DEPT and quantitative ^{29}Si NMR experiments for various ageing times at 100 °C (Table 1) shows a good agreement within the accuracy of the method. Accordingly, ^{29}Si DEPT NMR data can be considered quantitative in this peculiar case and kinetic profiles of the various T^n species can be extracted from the ^{29}Si DEPT NMR experiments. They are presented in the Figure 5.

Time	T^0		T^1		T^2		T^3	
	D	Q	D	Q	D	Q	D	Q
5h	1.2	0.0	21.4	20.6	64.1	66.0	13.2	13.4
9h	0.0	0.0	9.5	6.5	67.2	65.6	23.2	27.9
24h	0.0	0.0	2.8	2.0	50.3	50.5	46.9	47.6
48h	0.0	0.0	1.4	0.8	35.7	35.7	62.9	63.5
380h	0.0	0.0	1.0	0.5	15.3	14.7	83.7	84.8

Table 1. Comparison of the T^n relative amounts determined in ^{29}Si DEPT (D) or quantitative inverse gated decoupling (Q) ^{29}Si NMR experiments for various ageing times at 100 °C.

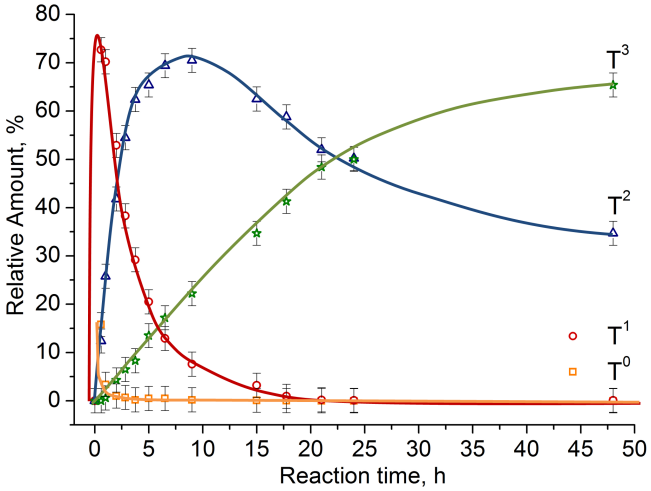

Figure 5. Evolution of the amount of T^n species during reaction at 100 °C for McPTMS/PrOH/ClAA/DBTL in a 1:18:6:0.015 ratio.

^{1}H NMR spectra, obtained between 0.5 and 380 hours of reaction at 100 °C, also bring information on the evolution of the system. The ^{1}H NMR spectrum for 24h hours is presented as an example in Figure 6. A full assignment of the signals has been performed with the help of ^{1}H-^{13}C HSQC and HMBC, as well as ^{1}H-^{29}Si HSQC or HMBC. ^{1}H NMR confirmed the transalcoholysis (reaction b), already observed by ^{29}Si NMR (Figure 2), and also the formation of propyl chloroacetate and methyl chloroacetate.

^{1}H NMR has also evidenced a partial loss of –SH functionality after *ca.* 20 hours of reaction at 100 °C, as can be seen in the zoom insertion for higher reaction times in Figure 6. A new signal, labeled g2, appears at slightly higher chemical shift than signal g1 (HS-C***H***$_2$-). As ^{1}H-^{13}C HMBC clearly shows a correlation of this new signal with a ^{13}C signal in the carbonyl region (*ca.* -170 ppm), this g2 signal was attributed to the gamma protons of the chlorothioacetate derivatives of propylsilane: $ClCH_2$-C(O)S-C***H***$_2$-CH_2-CH_2-SiO_3. These species are either formed by a direct reaction between McPTMS derivatives with free ClAA, or via transesterification reactions between McPTMS derivatives and propyl chloroacetate or methyl chloroacetate. This loss of –SH functionality is about 10% at 80 hours and reaches 40% after 380 hours at 100 °C. The formation of these parasitic species is clearly activated by temperature. Sols prepared at 100 °C for 80 hours and then stored for 90 days at 5°C do not show any evolution of their g1 and g2 signals, and exhibit an identical amount (90%) of –SH functionality in the fresh and stored sols.

As in situ water formation, used in this work, depends on the kinetics of the esters formation, ^{1}H NMR analysis was used to determine the amount of water produced for each reaction time. Deconvolution of the overlapping components attributed to ClAA (e), methyl chloroacetate (e') and propyl chloroacetate (e"), as shown in Figure 7, allowed to quantify these compounds and derived the amount of produced water ($A(H_2O)$) for a given reaction time, from equation 1 in which e, e' and e" represent the integral of each signal.

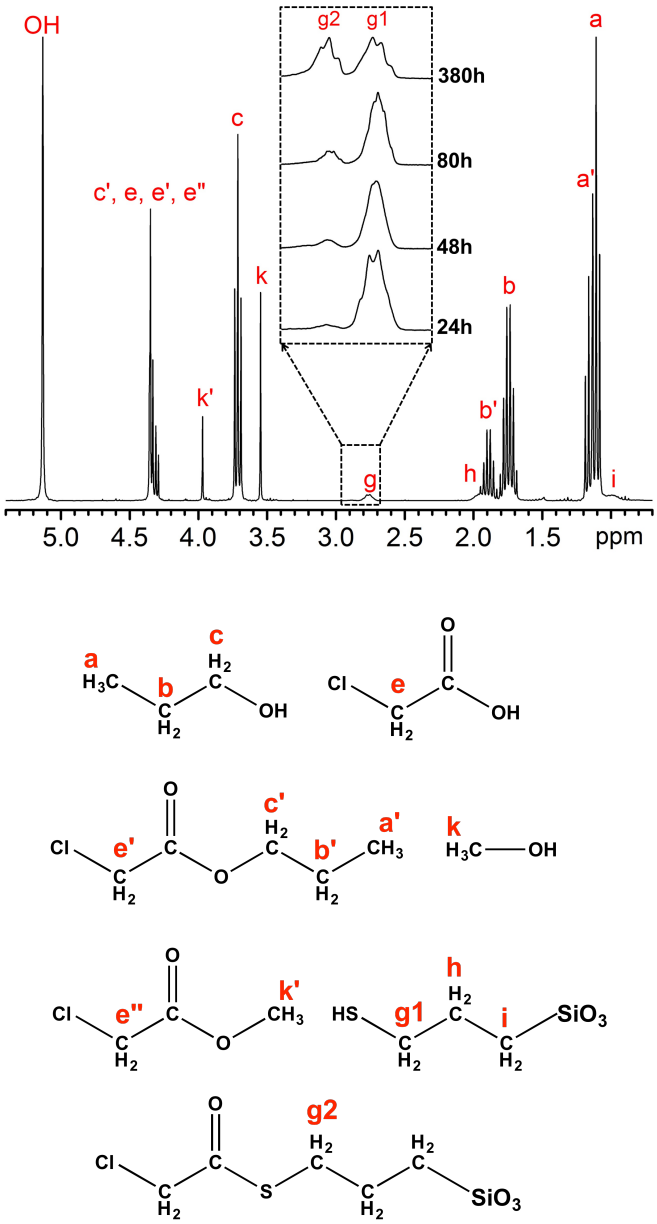

Figure 6. ^{1}H NMR spectrum and assignments after 24 hours of reaction at 100 °C. Zoom on the signals labelled g (S-C**H**$_2$-) for increasing reaction times (24, 48, 80, 380 hours).

$$A(H_2O) = \frac{1}{2} * e'/(\frac{e + e' + e"}{12}) + \frac{1}{2} * e"/(\frac{e + e' + e"}{12}) \qquad (1)$$

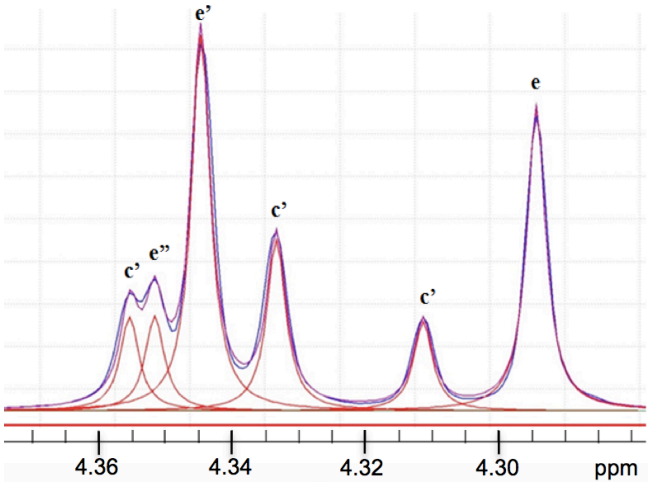

Figure 7. Deconvolution of the ^{1}H NMR spectrum zones used to derive the amount of water generated in situ (as prepared sol with a D_2O capillary).

The kinetics of water production is presented in Figure 8 for both temperature conditions. They compared very well with the time evolution of the degree of condensation (DOC) that can be computed from ^{29}Si NMR data with the formula displayed in equation 2. This good match emphasizes the relation that exists between the extent of water availability and condensation.

$$DOC = \frac{T^1 + 2 * T^2 + 3 * T^3}{3 * (T^0 + T^1 + T^2 + T^3)} * 100 \qquad (2)$$

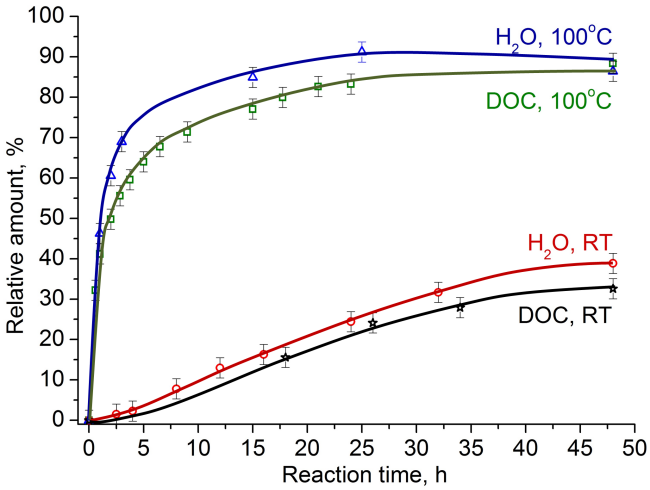

Figure 8. Kinetics of the in-situ water production and degree of condensation (DOC) determined for the sols at different times of reaction for McPMS/PrOH/ClAA/DBTL in a 1:18:6:0.015 ratios.

Water is continuously produced at room temperature by the esterification reaction and reaches only a maximum amount of 45 % of the theoretical value (*i.e.* H_2O/Si = 6) after 80 hours. This rather low production of water results in a poor condensation of the siloxane network with only a small amount of T^2 and almost no T^3 species. On the contrary, the sol-gel reaction at 100 °C leads already after 1 h to the availability of about the same amount of water. After 24 h the water production reaches its maximum (about 90% of the theoretical value). The high temperature conditions (Figure 5) increase strongly the hydrolysis-condensation capability, with only few % of residual monomer found after 1 h. The structural recombination of T^2 into T^3 species after longer reaction times is noteworthy and ^{29}Si DEPT NMR spectra acquired after selected reaction times are presented on the Figure 9.

Owing to the vast number of species formed, their detailed attribution is complicated, but nevertheless the assignment of peak groups related to the typical structures can be attempted.

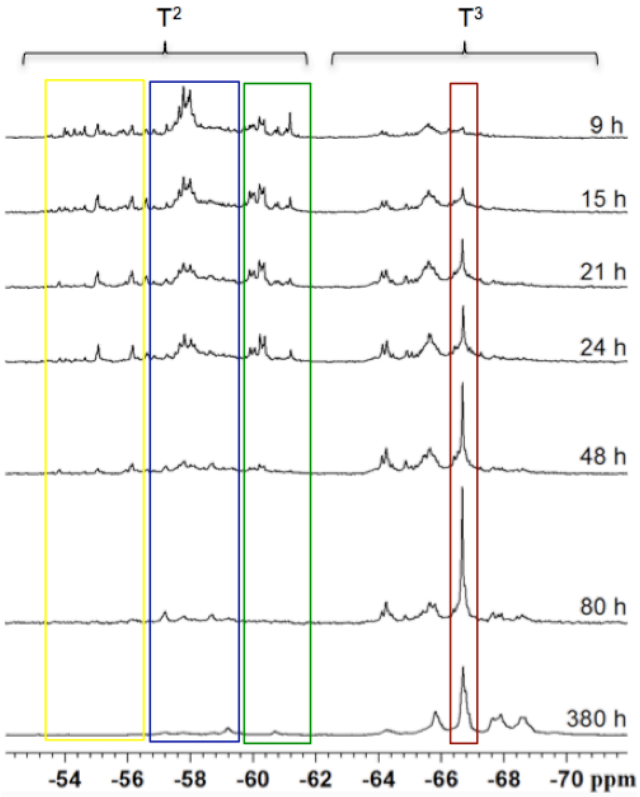

Figure 9. ^{29}Si DEPT NMR spectra of thiol functionalized NBBs in the T^2-T^3 region after selected reaction times at 100 °C.

Formation of cyclic species and their further rearrangement to more complex architectures is a known feature of silsesquioxanes polymerization under acidic conditions.[37,38] The ^{29}Si signals of the smaller $(RSi(OR')O)_n$ cyclic products ($n \leq 4$ and R'=Pr, Me, or H) show a lower field shift in comparison to the linear T^2, because the cyclization reduces the valence angles, decreasing density of positive charge on Si atoms.[39] The smaller cycles demonstrate lower field shift as a result of increasing internal tension, thus the sharp signals in the Figure 9 in the range -54 to -56.5 ppm (yellow) can be attributed to the most constrained $(T^2)_3$ cyclic units, bearing different alkoxy or –OH groups. This region contains also the T^2 signals associated to the condensed cyclic units $[(T^2)_2(T^3)]$ and $[(T^2)(T^3)_2]$. The group of resonances centered at -58 ppm (blue) is due to $(RSi(OR')O)_4$ cycles. As each silicon can bear an OPr, OMe or OH moiety, and due to different possible isomerization of such species, this group of signals appears broad due to the overlapping of vast number of individual resonances. The net amount of $(RSi(OR')O)_4$ cycles in reaction solution increases from the first hours of reaction (see Figure 4), reaching the maximum by 9 hours, and then decreases gradually with a plateau in the range of 21-24 hours of reaction. The signals in the range from -59 to -61 ppm (green) can be attributed to the middle Si atoms of linear T^2 species, and also to $(RSi(OR')O)_n$ cycles (n=5, 6).[40] Detailed assignment of the species in green region is unclear due to the extensive amount of possible signals for these cycles.

The T^3 region is composed of five groups of peaks, where the two overlapped peaks around -64.2 ppm can be attributed to the signals of ladder-like and T_6 cage-like species. Both species are likely formed by the cycles, detected in the T^2 region, that can build this type of structures in one step.[40] The signals centered at -65.6 ppm can be assigned to $(T^3)_4T^2(X)T^2(Y)T^2(Z)$ species (where X, Y, Z can be OPr, OMe or OH). Such species can also be described as the T_8 cages with one Si atom missing. The sharpest signal at -66.7 ppm (red) belongs to closed T_8 cages, as reported previously,[36] and since it is well known that the half-peak width decreases with increase in regularity of the species skeleton.[40] The corresponding signal appears well visible in the spectra collected after 9 hours of reaction, grows gradually until the plateau in the range of 21-24 hours of reaction and reaches the maximal intensity and minimal half-peak width by 80 hours. It is noteworthy, that detection of T_8 cages starts simultaneously

with reduction of $(RSi(OR')O)_4$ cycles net amount and also respects the 21-24 hours growth plateau. Contrariwise to $(RSi(OR')O)_4$ cycles, the net amount of other T^2 species changes negligibly in the time range 9-21 hours. Considering the high chemical stability of the $(RSi(OR')O)_4$ cycles,[40] they most probably directly rearrange into the T_8 cages. Such rearrangement starts when the amount of water produced in situ reaches 75% of the theoretical value, which can be considered as the transformation threshold value.

New groups of signals centered at -67.8 ppm and -68.6 ppm appear in T^3 region after 24 hours of reaction. According to Laine, the ^{29}Si NMR resonance associated to the T_{10} cage is located 0.7 ppm at lower frequencies than the one of the T_8 cage (i.e. *ca* -67.4 ppm) and the ^{29}Si NMR resonances associated to the T_{12} cage are 0.5 and 2.3 ppm at lower frequencies than the one of the T_8 cage (i.e. ca -67.2 and -69.0 ppm).[41] These proposed values match well the one observed here. However, for Ervithayasuporn, the shifts to lower frequencies are larger (1.9 ppm for the T_{10} resonance and 1.6 and 4.3 ppm for the T_{12} resonances),[42-44] which in our case would result in a T_{10} cage around -68.6 ppm and T_{12} cages around -68.3 and -71.0 ppm. It seems therefore difficult to exactly assigned these two new groups of signals, but they likely correspond to higher member cages (T_{10}, T_{12} and other bigger and less symmetrical polyhedral structures). Moreover, contrary to T_8 cages the mechanism of these species formation cannot be pointed out clearly.

By 380 hours of reaction, a broadening of all signals is observed. The branching or co-condensation of incompletely condensed cages may result in the formation of poly-cage structures with higher molecular weights. As a result, restricted mobility of such species, increase in reaction solution viscosity, as well as the substantial number of possible structural combinations can be the main reasons of observed signals broadening. Apart from that, the signal attributed to the ladder-like species (-64.2 ppm) almost disappears by 380 hours of reaction, suggesting the ladders rearrangement into polyhedral structures.

To confirm the species identification, FT-IR measurements were performed on as-made sols after various reaction times at 100 °C (Figure 10). Spectra indicate that Si–O–Si links are well formed via the condensation of McPTMS, as shown by intense and broad bands in the region between 950 and 1200 cm^{-1}. The band at 1033 cm^{-1} that can be attributed to the open chains,[26] is visible at the early stages of reaction, but begins to fade already after 6 hours of reaction. The bands at 1095 cm^{-1} and at 1067 cm^{-1} can be attributed to $(T^1)_2(OH)_4$ and ladder-like species respectively. However, it appears that strong bands at 1097 cm^{-1} and 1053 cm^{-1} of 1-propanol, highly abundant in sols, contribute to the same region, complicating the analysis. The band at 996 cm^{-1}, attributed to $(T^3)_4(T^2)_2(OH)_2$ open cages, shows the gradual intensification of related shoulder after 24 hours of reaction. The band centered at 1135 cm^{-1} can be attributed to T_8 cage-like species.[41] The amount of T_8 species increases starting from about 6 hours and reaches its maximum by 72 hours of reaction, when the corresponding peak experiences slight reduction of intensity and broadening.

The characteristic absorption of S-H stretching vibration is identified by a very weak and broad band at 2560 cm^{-1} (not shown). Accordingly, conclusions on –SH functions reactivity in produced NBBs and their decrease with time can only be inferred from ^1H NMR measurements (vide supra).

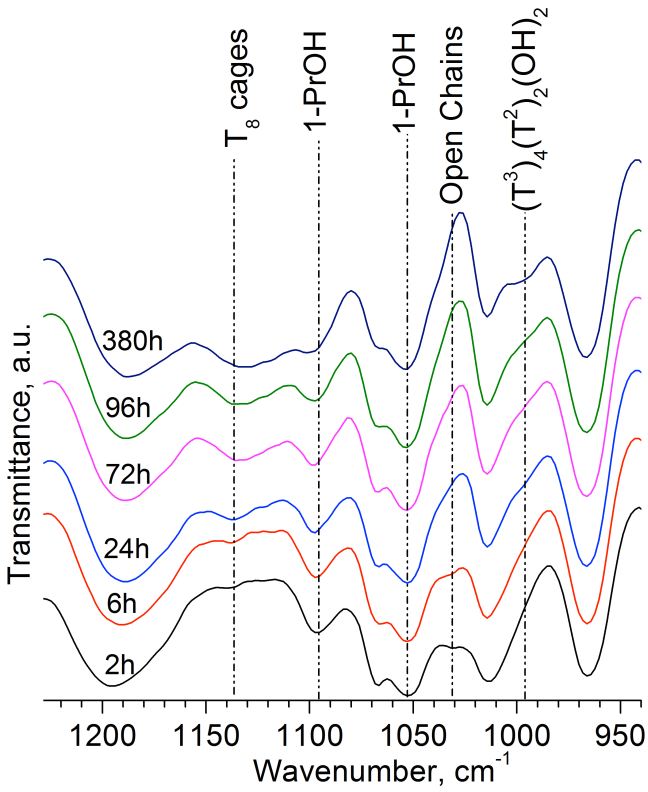

Figure 10. FTIR spectra of sols (McPTMS/PrOH/CLAA/DBTL 1:18:6:0.015) with increasing reaction time from 2 to 380 hours (bottom to top) at 100 ºC.

The evolution with reaction time of oligomers size distribution was evaluated by gel permeation chromatography (Figure 11). The retention volumes can be converted into equivalent molecular weights using polystyrene standards calibration. Yet, such a conversion can present some limitations on this type of systems, as previously reported.[39]

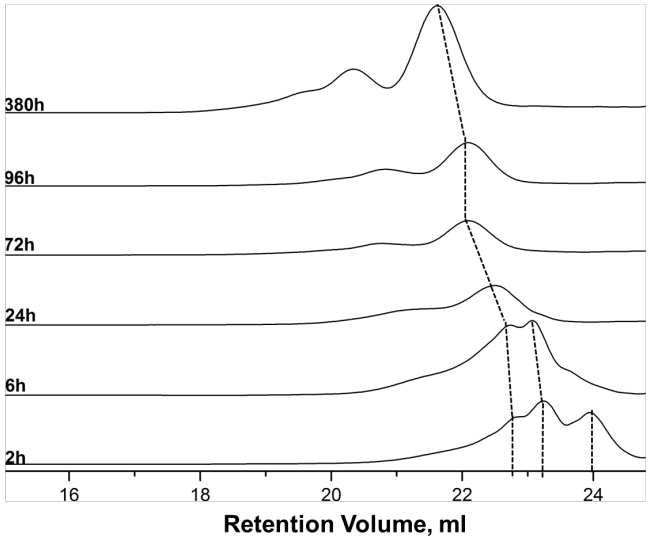

Figure 11. GPC traces of sols (McPTMS/PrOH/CLAA/DBTL 1:18:6:0.015) with increasing reaction time from 2 to 380 hours at 100 °C.

In agreement with FTIR and NMR, a variety of small oligomers are formed within the first 2 hours of reaction at 100 °C. These oligomers are distributed into three retention volumes: 23.95, 23.23 and 22.85 ml. After 6 hours of reaction, the GPC trace still shows three main families of species with smaller retention volumes (23.07, 22.73

and 21.37 ml), in agreement with the overall growth of the oligomers. After 24h of reaction, further growth and recombination lead to only two contributions: a major one at 22.50 ml and a minor one at 21.22 ml. Till 72 hours, these two contributions keep on growing to reach equivalent molecular weights of 760 and 1430 Da, corresponding to retention volumes of 22.10 and 20.77 ml, respectively. From 72 to 96 hours of reaction, the growth appears stopped, but after 380 hours the two main contributions in the GPC trace increase to 950 and 1770 Da, which correspond to retention volumes of 21.62 and 20.32 ml. The smaller species are likely associated to simple cage and ladder-like species, while the bigger ones might correspond to more complex poly-cage architectures.

The growth of the oligomers was also evaluated by ^{1}H PFG NMR (or DOSY NMR).[46] This technique measures translational diffusion coefficients, which can then be converted into hydrodynamic diameters with the well known Stokes-Einstein formula (Equation 3), where T is the temperature (298 K), k_B the Boltzmann constant (1.38 10^{-23} JK^{-1}), η the viscosity of the medium (0.501 cP for [D8]THF at 298 K[47]), and D_T the diffusion coefficient. This hydrodynamic diameter is just an estimation of the size of the species as it merely corresponds to the diameter of a spherical object that would exhibit the same diffusion coefficient.

$$d_H = \frac{k_B T}{3\pi\eta D_T} \qquad (3)$$

These measures were performed in THF-d8, the deuterated version of the GPC solvent. To take into account a possible evolution of the viscosity caused by the siloxane oligomers, octakis(trimethylsiloxy)silsesquioxane (Q_8M_8) was added to each sample. A diffusion coefficient of 6.5 ± 0.1 10^{-10} m^2s^{-1}, was found in all the samples for the Si-CH_3 signal, around 0 ppm, associated to Q_8M_8. This value corresponds to a hydrodynamic diameter of 1.34 nm, in good agreement with the molecular dimensions of Q_8M_8, which is a globular and isotropic entity. Because of strong overlapping with resonances related to propanol or propyl chloroacetate (Figure 6), the signals h and i of the siloxane species could not be confidently analyzed. Only the results obtained for signals g1 and g2 are reported in Table 2 as normalized diffusion coefficients, *i.e.* ratios of a diffusion coefficient by the diffusion coefficient of Q_8M_8. The corresponding hydrodynamic diameters are also given in Table 2.

Ageing (h),	Normalized D_T		d_H, (nm)	
100 °C	g1	g2	g1	g2
24	0.84	(a)	1.57	(a)
72	0.78	0.73	1.69	1.81
80	0.78	0.74	1.69	1.78
96	0.78	0.73	1.69	1.81
380	0.72	0.73	1.83	1.81

Table 2. Normalized D_T and hydrodynamic diameters $\boldsymbol{d_H}$ of species corresponding to **g1** (2.73 ppm) and **g2** (2.84 ppm) resonances by ^{1}H DOSY NMR in THF-d8 at T=298K. (a): too weak signal to be analyzed.

The attenuation profiles measured at each studied reaction time were always mono-gaussian and, accordingly, only one diffusion coefficient was necessary to describe each species at a given reaction time. This result might appear contradictory to GPC, which evidenced two main populations above 24 hours, but the resolution by DOSY of two diffusive components in a single signal is known to be rather difficult, especially when they differ by a factor lower than two.[46] Analysis of the DOSY results was therefore mainly focused on their evolution with the reaction time. While the normalized diffusion coefficient measured for g1 decreases from 0.84 to 0.72, when the reaction time goes from 24 to 380 hours, the one associated to g2 appears rather constant at 0.73. It seems therefore that the chlorothioacetate siloxane derivative, $ClCH_2C(O)SCH_2CH_2CH_2SiO_3$, is mostly formed with the larger oligomers (i.e. smaller diffusion coefficients). The evolution observed for signal g1 corresponds to a rather small change in hydrodynamic diameter: from 1.57 to 1.83 nm, i.e. by a factor of *ca.* 1.16. The factor is even smaller (~1.08) when considering the evolution from 72 to 380 hours. This small evolution corresponds however to a change in volume

by a factor of ~1.26 (*i.e.* 1.08^3). This factor is in good agreement with the equivalent mass evolution measured by GPC between 72 and 380 hours, which corresponds to a factor of 1.23-1.24 for both populations (vide supra). This good match seems also to indicate that the formed NBBs are rather globular (Mw α d_H^3). DOSY NMR results also confirm the growth plateau observed by GPC between 72 and 96 h of reaction time.

It is worth of noting that, apart from the stability of thiol function during storage (vide supra), the NBBs oligomers stored in as-made sols for 90 days at 5 °C did not show any structural evolution and retained their average molecular weights. Such stability can be an asset for further processing for desired applications. Indeed, the NBBs after different reaction times (24, 48, 80 and 380 hours) were tested for coating applications before and after their storage. All sampled sols demonstrated good filming ability on both soda lime glass and pure silicon substrates, resulting in smooth featureless coatings, prepared by spin-coating technique.

Conclusions

This study investigates the complex kinetics of growth of the thiol-functionalized Nanobuilding Blocks (NBBs). ISWP route was exploited for the sol-gel preparation of NBBs. In this route, the water provided in situ by the esterification reaction of chloroacetic acid and 1-propanol enabled the hydrolysis-condensation of 3-mercaptopropyltrimethoxysilane (McPTMS). ^{1}H NMR, ^{29}Si NMR, ^{1}H DOSY NMR, Gel Permeation Chromatography and FTIR were jointly applied for the characterization of sols. Despite a rich number of species formed at early ages, we were able to characterize structural units growth and recombination during the reactions. Optimization of the hydrolysis-condensation extent was explored by time-dependent monitoring of different temperature conditions reactions: room temperature and 100 ºC. It was shown, that the Si network structural features can be tuned by simply controlling the reaction duration. The water generated during the reaction was derived from ^{1}H NMR spectra fitting. Paired with the degree of condensation of NBBs, it demonstrated that hydrolysis-condensation rate follows the in situ water production trends versus reaction time. It was found, that after reaching a threshold value of the water availability in the reaction mixture (75% of theoretical value with exploited conditions), the cyclic species of Si network tend to directly rearrange into the cage-like species. –SH functions availability in the final material was evaluated by ^{1}H NMR, showing that 10% of -SH functionality has disappeared by 80 hours of reaction at 100 ºC, when the NBBs were represented mainly by cage-like oligomers and ladder-like species. The combination of gel permeation chromatography with ^{1}H DOSY NMR gave two different looks at the NBBs growth process and seems to suggest that the NBBs exhibit a globular architecture.

Experimental Section

1. Materials and reagents

3-mercaptopropyltrimethoxysilane (McPTMS), dibutyltin dilaurate (DBTL) were purchased from ABCR and used without any further purification. Chloro-acetic acid (ClAA), 1-propanol (PrOH), octakis(trimethylsiloxy)silsequioxane (Q_8M_8), and NMR deuterated solvents ([D8]THF, $CDCl_3$ and D_2O) were purchased from Sigma-Aldrich and used as received.

2. Synthesis of thiol-functionalized NBBs

The synthesis of the thiol-functionalized nanobuilding blocks (NBBs) was performed in nitrogen atmosphere using Schlenk technique. All solvents were dried before use, following standard procedures.[48] All the glassware used for reactions was dried in oven at 80 °C for 24 hours prior to use. 465 µl of McPTMS (2.5 mmoles, 1 eq.) was diluted in PrOH (3.36 ml, 18 eq.) in a self-condensing Schlenk flask. ClAA (1.417 g, 6 eq.) and the condensation promoter DBTL (22 µl, 0.015 eq.) were then added to the solution under vigorous stirring. The clear solution was left reacting at room temperature or 100 °C for different times. The reaction solution kept its initial transparency and homogeneity, and no precipitate was ever observed after all analyzed reaction times at both room temperature and 100 °C conditions.

3. Characterization Techniques

The **FT-IR** spectra of as-made solutions were recorded on a Thermo Optics Avatar 330 instrument, in transmission mode in the range 4000 to 400 cm^{-1} using KRS-5 windows (256 scans, 4 cm^{-1} resolution).

Gel Permeation Chromatography (**GPC**) traces were recorded with a Knauer system (Smartline Pump 1000 and RI detector 2300) completed with Polymer Laboratories-Varian PLgel 5 µm MIXED-C columns (7.5 x 300 mm). Samples of reaction solutions were injected (20 µl) and pumped through the columns with THF as mobile phase (flow-rate: 1 ml·min^{-1}). The calibration curve was measured using polystyrene standards (Polymer Laboratories) with Mw ranging from 580 to 100000 Da.

Solution ^{29}Si **NMR** spectra were collected on a Bruker Avance^{III} 400 instrument (400.13 and 79.49 MHz, for ^{1}H and ^{29}Si, respectively) equipped with a 10 mm BBO probe. Sols were analyzed as prepared in 10 mm NMR tubes with just a 3 mm D_2O coaxial capillary inserted for the lock. ^{29}Si-{^{1}H} NMR spectra were mainly acquired with a DEPT (Distortionless Enhancement by Polarization Transfer) sequence using the following experimentally adjusted parameters: evolution period (1/2J) of 55 ms (*i.e.* an equivalent coupling of *ca.* 9 Hz), 3rd ^{1}H pulse of 33°, and recycling delay of 4 s. Spectra with a good signal-to-noise ratio were obtained within 30 min, allowing to properly monitor the species along the ageing time. Quantitative ^{29}Si-{^{1}H} NMR experiments, using inverse gated decoupling to avoid NOE, were also acquired for selected reaction times (5, 9, 24, 48 and 380 h) with the following parameters: pulse angle of 30°, acquisition and decoupling time of *ca.* 0.75 s, and recycling delay of 10 s (much larger than the decoupling time). Spectra with a good signal-to-noise ratio were obtained in 4h. The ^{29}Si chemical shifts are referenced to tetramethylsilane (TMS) and the silicon units are labeled according to the usual notation: T^n where T represents $SiCO_3$ units and n the number of siloxane bridges.
^{1}H, ^{1}H-^{n}X (^{13}C or ^{29}Si) and ^{1}H DOSY NMR experiments were recorded on a Bruker Avance^{III} 300 spectrometer (300.13, 75.47 and 59.62 MHz for ^{1}H, ^{13}C and ^{29}Si, respectively) using a 5 mm BBFO probe equipped with a z-gradient coil providing a maximum gradient strength of 49.7 G.cm^{-1}. Deuterated solvents were added in various amounts to the solutions to analyze or, alternatively, a D_2O capillary was introduced in the 5 mm NMR tube. All experiments were performed, at 25°C. ^{1}H-^{n}X HSQC (Hetero Single Quantum Correlation) and HMBC (Hetero Multiple Bond Correlation) 2D experiments were performed with standard pulse sequences from the Bruker library (hsqcetgp and hmbcetgpnd). The delays in the sequences were set for coupling constants of 145 and 5 Hz for ^{1}H-^{13}C HSQC and HMBC, respectively, and 9 Hz for ^{1}H-^{29}Si HSQC or HMBC. ^{1}H DOSY NMR experiments[46] were performed with a double stimulated echo (dstebpgp3s) to compensate possible convection artifacts.[49] Sine shaped bipolar gradient pulses and an eddy current delay of 5 ms were used. The gradient amplitude was varied, in 32 increments, from 2 to 90% of the maximum gradient strength. The diffusion delays and gradient pulses length were in the range 100 – 600 ms and 0.7 – 2.0 ms, respectively. They were set to achieve an attenuation of *ca.* 95% for the signals of interest at the higher gradient strength. 50 µl of as prepared sols were diluted into 700 µl of [D8]THF and 5 to 10 mg of Q_8M_8 was added as an internal reference.[50]
^{1}H chemical shifts are referenced to TMS, using the signals of the protonated impurities of the solvents as secondary references (7.26, 4.70, 1.72 and 3.58 for $CDCl_3$, D_2O and [D8]THF, respectively [58]).
All NMR data processing and treatments (integration, fitting, deconvolution, and analysis of DOSY attenuation profile,) were performed with Topspin 3.1, the Bruker built-in software package.

Acknowledgements

The authors thank MIUR (PRIN 2009) for the financial support. This research is performed in the frame of MP1202 COST Action **"**Rational design of hybrid organic**–**inorganic interfaces: the next step towards advanced functional materials".

Keywords: sol-gel process, kinetics, NMR spectroscopy, Oligosilsesquioxanes

References

[1] C. Sanchez, G. Soler-Illia, F. Ribot, T. Lalot, C. Mayer, V. Cabuil, *Chem. Mater.* **2001**, *13*, 3061–3083.
[2] C. Sanchez, P. Belleville, M. Popall, L. Nicole, *Chem. Soc. Rev.* **2011**, *40*, 696–753.
[3] L. Nicole, C. Laberty-Robert, L. Rozes, C. Sanchez, *Nanoscale* **2014**, *6*, 6267–6292.
[4] P. Gómez-Romero, C. Sanchez, *Functional Hybrid Materials, Vol. 1 (Eds.* P. Gómez-Romero, C. Sanchez*), Wiley-VCH, Weinheim,* **2003**, pp. 1–14.
[5] G. Kickelbick, *Hybrid Materials, Vol. 1 (Eds. G. Kickelbick),Wiley-VCH, Weinheim,* **2007**, pp. 1–517.

[6] T. Ogasawara, A. Yoshino, H. Okabayashi, C. O'Connor, *Colloids Surfaces A Physicochem. Eng. Asp.* **2001**, *180*, 317–322.
[7] F. Beari, M. Brand, P. Jenkner, R. Lehnert, H.J. Metternich, J. Monkiewicz, H.W. Siesler, *J. Organomet. Chem.* **2001**, *625*, 208–216.
[8] A. Jitianu, A. Britchi, C. Deleanu, V. Badescu, M. Zaharescu, *J. Non. Cryst. Solids* **2003**, *319*, 263–279.
[9] R. Liu, Y. Xu, D. Wu, Y. Sun, H. Gao, H. Yuan, F. Deng, *J. Non. Cryst. Solids* **2004**, *343*, 61–70.
[10] B. Orel, R. Ješe, U. Lavrenčič Štangar, J. Grdadolnik, M. Puchberger, *J. Non. Cryst. Solids* **2005**, *351*, 530–549.
[11] M.-C. Brochier Salon, M. Abdelmouleh, S. Boufi, M.N. Belgacem, A. Gandini, *J. Colloid Interface Sci.* **2005**, *289*, 249–261.
[12] S. Torry, A. Campbell, A. Cunliffe, D. Tod, *Int. J. Adhes. Adhes.* **2006**, *26*, 40–49.
[13] H. Jiang, Z. Zheng, J. Xiong, X. Wang, *J. Non. Cryst. Solids* **2007**, *353*, 4178–4185.
[14] M.-C. Brochier Salon, M.N. Belgacem, *Colloids Surfaces A Physicochem. Eng. Asp.* **2010**, *366*, 147–154.
[15] O. Paquet, M.-C. Brochier Salon, E. Zeno, M.N. Belgacem, *Mater. Sci. Eng. C* **2012**, *32*, 487–493.
[16] A. Rauter, L. Slemenik Perše, B. Orel, B. Bengű, O. Sunetci, A. Šurca Vuk, *J. Electroanal. Chem.* **2013**, *703*, 97–107.
[17] A. Letailleur, F. Ribot, C. Boissière, J. Teisseire, E. Barthel, B. Desmazières, N. Chemin, C. Sanchez, *Chem. Mater.* **2011**, *23*, 5082–5089.
[18] U. Lavrencic Stangar, A. Sassi, A. Venzo, A. Zattin, B. Japelj, B. Orel, S. Gross, *J. Sol-Gel Sci. Technol.* **2009**, *49*, 329–335.
[19] M.-C. Brochier Salon, P.-A. Bayle, M. Abdelmouleh, S. Boufi, M. Belgacem, *Colloids Surfaces A Physicochem. Eng. Asp.* **2008**, *312*, 83–91.
[20] L. Yang, J. Feng, W. Zhang, J. Qu, *Appl. Surf. Sci.* **2010**, *257*, 990–996
[21] A.J. Burggraaf in *Fundamentals of Inorganic Membranes and Technology* (Ed.: A. J. Burggraaf, L. Cot), Elsevier, **1996** (Membranes Science and Technology, vol. 4), pp. 331–443.
[22] F. Mammeri, C. Bonhomme, F. Ribot, F. Babonneau, S. Dirè, *Chem. Mater.,* **2009***, 21,* 4163–4171.
[23] U. Schubert, *Acc. Chem. Res.* **2007**, *40*, 730–737.
[24] S. Dirè, P. Egger, M.L.D. Vona, M. Trombetta, S. Licoccia, *J. Sol-Gel Sci. Technol.* **2004**, *32*, 57–61.
[25] R. Di Maggio, S. Dirè, E. Callone, F. Girardi, G. Kickelbick, *Polymer,* **2010**, *51*, 832–841.
[26] V. Tagliazucca, E. Callone, S. Dirè, *J. Sol-Gel Sci. Technol.* **2011**, *60*, 236–245.
[27] E. Borovin, E. Callone, B. Papendorf, G. Guella, S. Dirè, *J. Nanosci. Nanotechnol.* **2015**, doi:10.1166/jnn.2016.11031.
[28] A.C. Pierre, *Biocatal. Biotransformation* **2004**, *22*, 145–170.
[29] B. Hendan, H. Marsmann, *Appl. Organomet. Chem.* **1999**, *13*, 287–294.
[30] J. Anker, P. Hall, O. Lyandres, N. Shah, J. Zhao, R. Van Duyne, *Nat Mater* **2008**, *7*, 442–453.
[31] F. Zamborini, L. Bao, R. Dasari, *Anal. Chem.* **2012**, *84*, 541–576.
[32] F. Brunet, *J. Non. Cryst. Solids* **1998**, *231*, 58–77.
[33] J. Pouxviel, J. Boilot, J. Beloeil, J. Lallemand, *J. Non. Cryst. Solids* **1987**, *89*, 345–360.
[34] L. Malier, F. Devreux, F. Chaput, J. Boilot, *Phys. Rev. A* **1992**, *46*, 959–962.
[35] R. Hook, *J. Non. Cryst. Solids* **1996**, *195*, 1–15.
[36] J. Fu, L. Shi, Y. Chen, S. Yuan, J. Wu, X. Liang, Q. Zhong, *J. Appl. Polym. Sci.* **2008**, *109*, 340–349.
[37] F. Brunet, B. Cabane, *J. Non. Cryst. Solids* **1993**, *163*, 211–225.
[38] A. Vainrub, F. Devreux, J. Boilot, F. Chaput, M. Sarkar, *Mater. Sci. Eng. B* **1996**, *37*, 197–200.
[39] L. Matějka, O. Dukh, J. Brus, W. Simonsick Jr, B. Meissner, *J. Non. Cryst. Solids* **2000**, *270*, 34–47.
[40] M. Itoh, F. Oka, M. Suto, S. D. Cook, N. Auner, *Int. J. of Polym. Sci.* **2012**, Article ID 526795, 1–17.
[41] J. Furgal, J. H. Jung, T. Goodson, R. Laine, *J. Am. Chem. Soc.* **2013**, *135*, 12259–12269.
[42] T. Jaroentomeechai, P. Yingsukkamol, C. Phurat, E. Somsook, T. Osotchan, V. Ervithayasuporn, *Inorg. Chem.* **2012**, *51*, 12266–12272.
[43] V. Ervithayasuporn, S. Chimjarn, *Inorg. Chem.* **2013**, *52*, 13108–13112.
[44] S. Chimjarn, R. Kunthom, P. Chancharone, R. Sodkhomkhum, P. Sangtrir-utnugula, V. Ervithayasuporn, *Dalton Trans.* **2015**, *44*, 916–919.
[45] E. Park, H. Ro, C. Nguyen, R. Jaffe, D. Yoon, *Chem. Mater.* **2008**, *20*, 1548–1554.
[46] C. Johnson Jr., *Prog. Nucl. Magn. Reson. Spectrosc.* **1999**, *34*, 203–256.
[47] M. Holz, X. Mao, D. Seiferling, A. Sacco, *J. Chem. Phys.* **1996**, *104*, 669–679.
[48] W. Armarego, *J. Organomet. Chem.* **1981**, *213*, 1–62.

[49] A. Jerschow, N. Müller, *J. Magn. Reson.* **1997**, *125*, 372–375.
[50] L. Van Lokeren, G. Maheut, F. Ribot, V. Escax, I. Verbruggen, C. Sanchez, J. Martins, M. Biesemans, R. Willem, *Chem. – A Eur. J.* **2007**, *13*, 6957–6966.
[51] G. Fulmer, A. Miller, N. Sherden, H. Gottlieb, A. Nudelman, B. Stoltz, J. Bercaw, K. Goldberg, *Organometallics* **2010**, *29*, 2176–2179.